Available online at www.sciencedirect.com

ScienceDirect

Physics Procedia 51 (2014) 46 – 49

Physics Procedia

ESS Science Symposium on Neutron Particle Physics at Long Pulse Spallation Sources, NPPatLPS 2013

Beam line parameters for PERC at the ESS

Christine Klauser[a,b,*], Hartmut Abele[b], Torsten Soldner[a,*]

[a] Institut Laue-Langevin, 6 rue Jules Horowitz BP 156, 38042 Grenoble CEDEX 9, France
[b] Atominstitut Technische Universität Wien, Stadionallee 2, 1020 Wien, Austria

Abstract

Precision measurements of correlations in neutron beta decay test the standard model of particle physics. Here, pulsed neutron beams are invaluable to fight systematic effects. We show that the Proton Electron Radiation Channel PERC in pulsed mode is particularly well suited for a long-pulse spallation source, due to its long decay volume. We indicate how the optimum beam line parameters to run PERC at the ESS can be derived and compare the performance with that at the most powerful continuous source, the reactor of the ILL.

© 2013 The Authors. Published by Elsevier B.V. Open access under CC BY-NC-ND license.
Selection and peer-review under responsibility of scientific committee of NPPatLPS 2013.

Keywords: Neutron beta decay; European Spallation Source; Proton Electron Radiation Channel; cold neutrons.

1. Introduction

The neutron decays into a proton, an electron and an anti-electron-neutrino. High-precision measurements of correlations between the decay products enable low-energy tests of the standard model, see e.g. [1]. The Proton Electron Radiation Channel PERC [2] is a new instrument designed to measure correlation coefficients in neutron decay with 10^{-4} accuracy. It uses a decay volume with $l = 8\,\mathrm{m}$ length and a cross section of $6 \times 6\,\mathrm{cm}^2$ made from a neutron guide. The charged decay particles are collected from the decay volume by a longitudinal magnetic field and separated from the neutron beam via a magnetic chicane. A magnetic mirror precisely defines the phase space of the particles to be detected. For details, see [2, 3].

Pulsed beams provide important information for systematic studies, as discussed for the instrument PERKEO III in [4]. For PERC, a pulsed beam is particularly important to study the magnetic mirror effect. The chopper would be installed directly in front of PERC, see Fig. 1. If the neutron beam is not monochromatic, the neutron pulse will spatially expand while travelling through the decay volume. In order to have a sufficiently localised neutron pulse, we request a pulse length p when the first neutrons reach the beam stop. For quantitative estimates we use $p = 2\,\mathrm{m}$, corresponding to the length of the guide sections in PERC. Furthermore, we request that the next pulse enters the decay volume once the previous one has completely left it. These two conditions together with the wavelength distribution in the pulse completely define the operation conditions of the chopper. At a continuous source, the

* Corresponding authors.
E-mail addresses: klauser@ill.fr (Christine Klauser). soldner@ill.fr (Torsten Soldner).

1875-3892 © 2013 The Authors. Published by Elsevier B.V. Open access under CC BY-NC-ND license.
Selection and peer-review under responsibility of scientific committee of NPPatLPS 2013.
doi:10.1016/j.phpro.2013.12.011

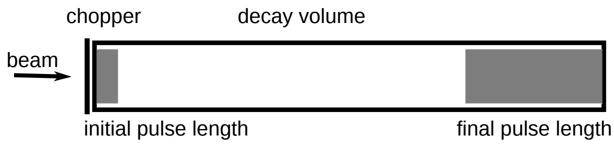

Fig. 1. Set-up for PERC in pulsed mode: A disk chopper is located directly in front of the decay volume. The spatial extension of the pulse increases over the course of its path.

wavelength distribution can be defined by a monochromator (crystal or velocity selector) in front of the chopper and is then independent of the chopper operation. At a pulsed source, the chopper unavoidably defines not only the time structure of the pulsed beam but also its wavelength distribution which requires to find the best compromise between wavelength bandwidth and chopper opening time.

In this paper, we show how to optimize beam parameters for PERC in pulsed mode at continuous and at pulsed sources. We compare the performances in terms of time-averaged flux. For numerical estimates we use the time structure of the ESS with the pulse length $2\tau = 2.86$ ms and the pulse frequency $f_{\mathrm{ESS}} = 14$ Hz [5] and a peak flux of 30 times the continuous flux of the ILL, $\Phi_{\mathrm{ESS}}^{\mathrm{Peak}}(\lambda) = 30\Phi_{\mathrm{ILL}}(\lambda)$, where Φ indicates differential capture fluxes (for definition see e.g. Eqn. (4) in [6]) in units of $[\mathrm{cm}^{-2}\mathrm{s}^{-1}\mathrm{\AA}^{-1}]$. We use $\lambda_0 = 5$ Å as reference wavelength. As λ_0 is close to the maximum of the capture flux spectrum and the considered wavelength distributions are small, we assume the flux to be wavelength-independent in the region of interest. We use l as distance between chopper and beam stop, ignoring potential gaps. Chopper opening and closing is assumed to be negligibly fast. We optimise for statistics only. The emphasis lies in the comparison of the two source types, absolute flux numbers will not be derived. Waiting times between two pulses or the omission of pulses that may be useful for systematic studies are not considered here.

2. Continuous Source

Wavelength selection and pulse definition can be achieved by a two-chopper system as proposed in [7]. The equations derived in Sec. 3 can be applied to this case. Here we discuss wavelength selection by a monochromator, in particular an idealized velocity selector with a triangular transmission function with 100% transmission for λ_0. The neutron wavelength spectrum is limited to the interval $(\lambda_{\min}, \lambda_{\max}) \equiv (\lambda_0 - \Delta\lambda, \lambda_0 + \Delta\lambda)$. The wavelength-integrated flux at the entrance of the chopper is then $\Phi_{\mathrm{ILL}}(\lambda_0)\Delta\lambda$. The space-time diagram is shown in Fig. 2 (a). At each time $t \in (-\vartheta, \vartheta)$ of the chopper opening, neutrons of the full wavelength band $(\lambda_{\min}, \lambda_{\max})$ traverse the chopper. The pulse

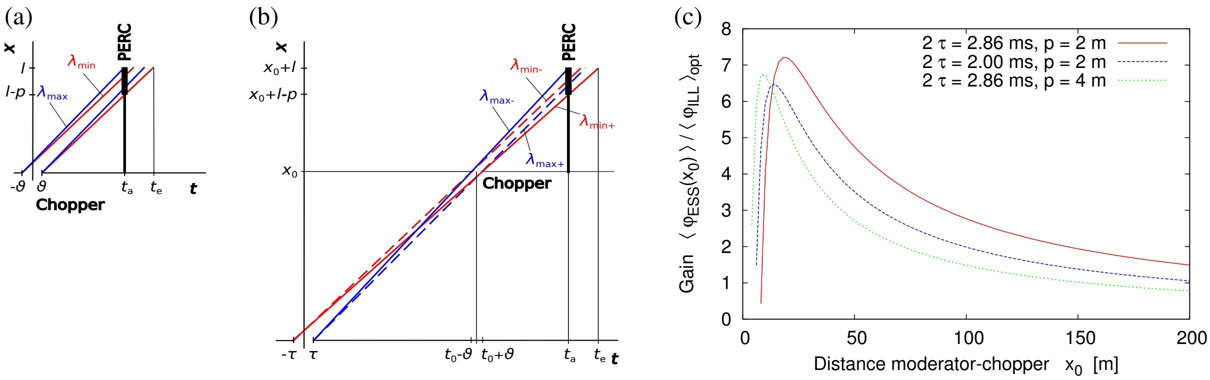

Fig. 2. (a) Space-time-diagram for a continuous source with monochromator. At each moment, the full wavelength band $(\lambda_{\min}, \lambda_{\max})$ arrives at the chopper. (b) Space-time-diagram for a pulsed source. The wavelength band $(\lambda_{\min}, \lambda_{\max})$ at x_0 depends on the time t and changes during the opening of the chopper. For the dimensioning of the chopper opening time, only the fastest neutrons $\lambda_{\min,-}$ at $t_0 - \vartheta$ and the slowest neutrons $\lambda_{\max,+}$ at $t_0 + \vartheta$ are important. (c) Gain factors for PERC at the ESS as function of distance to the moderator relative to the respective optimum at the ILL: for the standard parameters, for a reduced initial pulse length $\tau = 2$ ms (obtainable by a chopper at the moderator exit), and for a final pulse length of $p = l/2 = 4$ m with $\langle\varphi_{\mathrm{PERC,ILL}}\rangle_{\mathrm{opt}} = 0.147$ Å $\Phi_{\mathrm{ILL}}(\lambda_0)$.

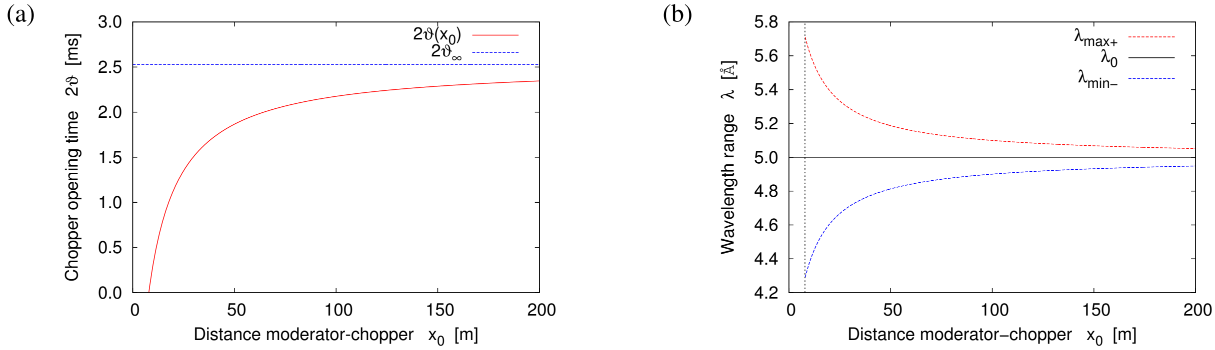

Fig. 3. (a) Chopper opening time for a 2 m pulse . (b) Minimum and maximum wavelength in a pulse for PERC at the ESS as function of distance. The vertical dashed line in (b) indicates the minimum distance $x_{0,\text{min}}$.

length $p(t)$ at time $t > \vartheta$ is given by the distance between the fastest neutrons that left the chopper at $-\vartheta$ and the slowest neutrons that left the chopper at ϑ. The condition $p(t_a) = p$ (where t_a is the arrival time of the fastest neutrons at the beam stop; t_e the time for the slowest ones) is fulfilled for:

$$2\vartheta = \frac{1}{k}\left(p\lambda_0 + \Delta\lambda(p-2l)\right) \quad \text{where we use} \quad \lambda v = k \equiv \frac{h}{m_n} = 3956\,\text{Å}\,\frac{\text{m}}{\text{s}} \quad (v \text{ is the neutron velocity}). \tag{1}$$

The one-pulse-at-a-time condition allows for the maximum chopper frequency f:

$$f = \frac{1}{t_e + 2\vartheta} = \frac{k}{\lambda_0(l+p) + \Delta\lambda(p-l)}. \tag{2}$$

The time-averaged flux in PERC is:

$$\langle\varphi_{\text{PERC,ILL}}\rangle = 2\vartheta f \Phi_{\text{ILL}}(\lambda_0)\Delta\lambda. \tag{3}$$

The optimum relative resolution $(\Delta\lambda/\lambda)_{\text{opt}}$ for the maximum flux can be calculated analytically and depends only on the ratio p/l. For the numerical values for PERC and our reference beam we obtain $(\Delta\lambda/\lambda)_{\text{opt}} = 7.3\%$ (achievable with a specially-designed selector), $2\vartheta_{\text{opt}} = 1.24\,\text{ms}$, $f_{\text{opt}} = 82.7\,\text{Hz}$, and $\langle\varphi_{\text{PERC,ILL}}\rangle_{\text{opt}} = 0.037\,\text{Å}\,\Phi_{\text{ILL}}(\lambda_0)$. For a standard selector with 10% resolution, the flux is $\langle\varphi_{\text{PERC,ILL}}\rangle_{10\%} = 0.032\,\text{Å}\,\Phi_{\text{ILL}}(\lambda_0)$.

3. Pulsed Source

At pulsed sources, the time structure limits the wavelength band arriving during the opening of a chopper at distance x_0: From all neutrons emitted at $t \in (-\tau, \tau)$ during the source pulse, only neutrons in the wavelength band $(\lambda_{\text{min}}(t), \lambda_{\text{max}}(t)) \equiv (k(t_0-t-\vartheta)/x_0, k(t_0-t+\vartheta)/x_0)$ are transmitted by the chopper with the opening interval $(t_0-\vartheta, t_0+\vartheta)$, where $t_0 = x_0\lambda_0/k$. The chopper thus not only defines the pulse length but also the bandwidth used. The wavelength band in one pulse has a constant width but changes from $(\lambda_{\text{min}-}, \lambda_{\text{max}-}) \equiv (k(t_0-\tau-\vartheta)/x_0, k(t_0+\tau-\vartheta)/x_0)$ to $(\lambda_{\text{min}+}, \lambda_{\text{max}+}) \equiv (k(t_0-\tau+\vartheta)/x_0, k(t_0+\tau+\vartheta)/x_0)$ from the beginning to the end of the chopper opening. The pulse length $p(t)$ in PERC at time $t > t_0 + \vartheta$ is given by the distance between the fastest neutrons $\lambda_{\text{min-}}$ entering PERC at $t_0 - \vartheta$ and the slowest neutrons $\lambda_{\text{max+}}$ entering at $t_0 + \vartheta$. The condition $p(t_a) = p$ is fulfilled if:

$$2\vartheta(x_0) = 2\frac{p(t_0+\tau) - 2l\tau}{2(x_0+l) - p}. \tag{4}$$

The condition for the pulse length can only be fulfilled for $x_0 > x_{0,\text{min}} \equiv k(2l-p)\tau/(p\lambda_0)$. For $x_0 \to \infty$, the chopper opening time converges to $2\vartheta_\infty = p\lambda/k$. The chopper opening time and minimum and maximum wavelength are plotted as function of distance in Fig. 3. The time-averaged flux depends on the distance to the moderator:

$$\varphi_{\text{ESS}}(x_0) = \int_{-\tau}^{\tau} \mathrm{d}t \left(\int_{\lambda_{\text{min}}(t)}^{\lambda_{\text{max}}(t)} \mathrm{d}\lambda \Phi_{\text{ESS}}(\lambda, t) \right) = 4 f_{\text{ESS}} k \frac{\tau\vartheta(x_0)}{x_0} \Phi_{\text{ESS}}(\lambda_0). \tag{5}$$

Fig. 2 (c) shows the gain factor that can be achieved by operating PERC at the ESS as function of the distance x_0. Note that the one-pulse-at-a-time condition would allow for a higher frequency:

$$f_{\mathrm{ESS}}^{\mathrm{opt}}(x_0) = \frac{1}{t_{\mathrm{e}} - t_0 + \vartheta} = \frac{1}{\vartheta(x_0)(2 + l/x_0) + l(\lambda_0/k + \tau/x_0)} \quad \text{with} \quad f_{\mathrm{ESS}\infty}^{\mathrm{opt}} \equiv f_{\mathrm{ESS}}^{\mathrm{opt}}(x_0 \to \infty) = \frac{1}{l\lambda_0/k + 2\vartheta_\infty}. \tag{6}$$

4. Discussion and Conclusions

At a continuous source, wavelength band and time structure can be chosen independently from each other by suitable monochromators and choppers, respectively. Therefore, the distance to the source is unimportant (neglecting losses in the neutron guide). In practice, large distances are preferable because of background and available space. In contrast, at a pulsed source a chopper unavoidably restricts the wavelength band. If one needs to limit the spatial length of a pulse the distance between source and experiment has to be chosen carefully. For short distances, the large bandwidth requires a short chopper opening time. For long distances, the chopper opening time is limited by $2\vartheta_\infty$ and the bandwidth reduces. For our example, the highest intensity is obtained for a distance of 19 m. A gain factor of 7 compared to a continuous source with the same time-averaged flux and a selector with optimum wavelength resolution can be achieved. The repetition rate of the ESS is fixed to 14 Hz. If the ESS would operate at the optimum frequency for PERC, $f_{\mathrm{ESS}}^{\mathrm{opt}} = 83$ Hz, the gain factor would be 43. This number is unequal to the peak flux factor 30 due to, on the one hand, the flux reduction by the triangular transmission function of the monochromator and, on the other hand, the fact that bandwidth and chopper opening can be chosen at the optimum for the continuous source.

The source pulse length 2τ can be reduced by installing a chopper at the moderator exit, see Fig. 2 (c). This reduces the bandwidth at a given distance and allows to increase 2ϑ but is profitable at very short distances only. Already the distance of 19 m is too short to provide enough lateral space and sufficient suppression of background from the source. However, at larger distances the gain compared to a continuous source is still substantial. A further gain in intensity is possible by opening the chopper several times per source pulse. The additional pulses have different wavelength bands and can be designed to fulfill both conditions. This allows to recover some of the time lost because of the low repetition rate of the ESS and may be particularly useful to master wavelength-dependent systematic effects.

An obvious parameter for optimisation is the final pulse length p. Increasing p allows to increase the wavelength band and the chopper opening time. For the continuous source and $p = 4$ m, we find $(\Delta\lambda/\lambda)_{\mathrm{opt}} = 17\%$ and $2\vartheta_{\mathrm{opt}} = 2.45$ ms, resulting in a flux gain of a factor 3.9 compared to $p = 2$ m, in spite of the slightly decreased chopper frequency $f_{\mathrm{opt}} = 70$ Hz. The gain for the ESS relative to the continuous source with optimum wavelength resolution is shown in Fig. 2 (c). Note that, as the optimum bandwidth is larger than for $p = 2$ m, the gain drops faster with distance. The substantially increased flux at both source types comes at the price of a worse localisation of the pulse and has to be balanced against the related systematic effects. Concerning a longer decay volume l, the bandwidth needs to be reduced in order to assure a sufficiently localised pulse. This favours longer distances from a pulsed source. Also the optimum pulse frequency reduces and thus approaches the operation frequency of the ESS. These arguments indicate that the gain factor at the ESS increases with the length of the decay volume.

We conclude that the long-pulse spallation source ESS will provide substantial gain factors for PERC-like instruments. A careful design of the beam line for particle physics is required to profit best from the time structure.

Acknowledgements: This work was supported by the priority program “Precision experiments in particle- and astrophysics with cold and ultra cold neutrons” (SPP1491, grant SO 1058/1-1) of the Deutsche Forschungsgemeinschaft.

References

[1] D. Dubbers, Physics Procedia (these proceedings).
[2] D. Dubbers et al., Nucl. Instr. and Meth. A 596 (2008) 238 – 247.
[3] G. Konrad et al., J. Physics: Conf. Series 340 (2012) 012048.
[4] B. Märkisch et al., Nucl. Instr. and Meth. A 611 (2009) 216 – 218.
[5] S. Peggs (ed.), ESS Technical Design Report, Tech. rep., ESS AB, Lund, `http://esss.se/documents/tdr/TDR_final.pdf` (April 2013).
[6] H. Abele et al., Nucl. Instr. and Meth. A 562 (2006) 407 – 417.
[7] D. Dubbers, Proceedings of the Workshop “Quark-Mixing, CKM-Unitarity”, Heidelberg 2002, Germany (2003) 67–69arXiv:hep-ph/0312124.